

## ORIGINAL RESEARCH ARTICLE

## Multi-scale mechanisms affecting fatigue properties of warm-mix recycled asphalt mixtures in Asian road engineering: Effects of freeze–thaw cycles and environmental synergies

Yu Wang<sup>1,2</sup> and Jiansan Hu<sup>3\*</sup><sup>1</sup>Equipment Material Technology Center, Inner Mongolia Electric Power Research Institute, Hohhot, Inner Mongolia Power (Group) Co., Ltd., Inner Mongolia Autonomous Region, China<sup>2</sup>Department of Hydraulic Engineering, College of Hydraulic and Environmental Engineering, China Three Gorges University, Yichang, Hubei, China<sup>3</sup>Department of Road and Bridge Engineering, College of Energy and Transportation Engineering, Inner Mongolia Agricultural University, Hohhot, Inner Mongolia Autonomous Region, China

## Abstract

Asia—one of the world's most densely populated regions—faces pressures from water scarcity, industrial pollution, and the environmental demands of infrastructure construction. Reclaimed asphalt pavement (RAP) technology, combined with warm-mix (WM) technology, is a key pathway toward achieving low-carbon road engineering and reducing resource consumption. However, research on the environmental adaptability of these technologies under Asian climatic conditions (e.g., frequent freeze–thaw cycles and prevalent salt-corrosion environments) remains insufficient. This study focuses on WM recycled asphalt mixtures (WMRAM) and innovatively introduces WM recycled asphalt mortar (WMRAMO) as the core medium. Using fatigue tests on WM recycled asphalt (WMRA), WMRAMO, and WMRAM and damage-mechanics indices, we systematically analyzed the effects of typical Asian environmental factors (freeze–thaw cycles, salt solution concentration) on fatigue performance. Results showed that under optimal WM recycling processes, WMRAM's fatigue performance outperformed traditional hot-mix asphalt mixtures, providing technical support for low-carbon road construction in Asia. Freeze–thaw cycles and salt solution concentration had markedly opposite effects on microcrack propagation and fatigue failure. Meanwhile, a high RAP content exacerbated initial microdamage, leading to unstable fatigue performance—this finding explains the core cause of discrepancies in existing research. A correlation between WMRAMO and WMRAM fatigue life, based on RAP content and loading strain, was established, enabling the prediction of WMRAM fatigue life through mortar-scale tests, offering a new method for material design in road engineering in cold regions of Asia. This research fills a gap in environmental synergy studies of WMRA technology under climatic conditions common in cold regions of Asia, providing a scientific basis for balancing infrastructure development and environmental protection.

**Keywords:** Warm-mix recycled asphalt mixture; Fatigue performance; Multi-scale analysis; Freeze–thaw cycles; Environmental synergies

**\*Corresponding author:**Jiansan Hu  
(huixiatao@163.com)

**Citation:** Wang Y, Hu J. Multi-scale mechanisms affecting fatigue properties of warm-mix recycled asphalt mixtures in Asian road engineering: Effects of freeze–thaw cycles and environmental synergies. *Asian J Water Environ Pollut.* 2026;23(3):025010399. doi: 10.36922/AJWEP025010399

**Received:** December 31, 2025**Revised:** January 12, 2026**Accepted:** January 14, 2026**Published online:** April 29, 2026

**Copyright:** © 2026 Author(s). This is an Open-Access article distributed under the terms of the Creative Commons Attribution License, permitting distribution, and reproduction in any medium, provided the original work is properly cited.

**Publisher's Note:** AccScience Publishing remains neutral with regard to jurisdictional claims in published maps and institutional affiliations.

## 1. Introduction

As two efficient low-carbon road construction technologies, waste asphalt mixture recycling and warm-mix asphalt technologies are of great significance in reducing carbon emissions, conserving energy, and protecting the environment.<sup>1</sup> For each 10 % increase in reclaimed asphalt pavement (RAP), material costs may decrease by 7%, CO<sub>2</sub> emissions by 3%, and energy consumption by 2%.<sup>2,3</sup> Compared with hot-mix asphalt, warm-mix asphalt can reduce energy consumption by 18–30% and pollutant emissions by 24%.<sup>4–6</sup> Our preliminary study (data now shown) has compared the harmful emissions of warm-mix recycled asphalt mixtures (WMRAM) and styrene–butadiene–styrene (SBS)-modified asphalt mixtures (SBSMAM), demonstrating that nitrogen oxides of WMRAM, compared to SBSMAM, were reduced by 3%, CO<sub>2</sub> by 30%, asphalt fume by 33%, and benzopyrene was almost reduced to 0 (primarily due to the reduction of construction temperature).

At present, the main reason limiting the widespread adoption of heat-tracing regeneration technology in asphalt mixture plants is the difficulty in increasing reclaimed asphalt pavement (RAP) content, which results in poor economic benefits.<sup>7–9</sup> The combination of warm-mix technology and regeneration technology of asphalt mixtures can solve this problem. While maintaining pavement performance, the hybrid approach can enhance RAP content and provide better construction workability.<sup>10,11</sup> As research has progressed, conclusions regarding the fatigue

performance of WMRAM have gradually diverged. For example, it has been shown that WMRAM has better high-temperature performance, fatigue performance, and water damage resistance than ordinary plant hot-mix recycled asphalt mixtures.<sup>12–14</sup> Conversely, other reports pointed out that WMRAM, with an organic warm-mix agent, has better water damage resistance but worse fatigue performance than hot-mix asphalt mixtures.<sup>5,15</sup> Tang *et al.*<sup>16</sup> found that with the increase of RAP content, the fatigue performance of WMRAM continuously decreased, whereas high-temperature performance, low-temperature performance, and water damage resistance initially increased and then decreased. Wang *et al.*<sup>17</sup> found that the fatigue performance of WMRAM is inferior to that of fresh asphalt mixtures but significantly better than hot-mix recycled asphalt mixtures. These findings, together with others,<sup>18,19</sup> indicate that the research conclusions of fatigue performance of recycled asphalt mixtures, especially WMRAM, are obviously inconsistent.

The fatigue research methods for asphalt and asphalt mixtures can be discussed from two aspects: test types and fatigue characterization. The types, advantages, and disadvantages of test methods are summarized in Table 1. Considering the advantages and disadvantages of several tests, this study used the linear amplitude sweep (LAS) test to evaluate the fatigue performance of warm-mix recycled asphalt (WMRA), and the four-point bending fatigue test to assess the fatigue performance of WMRA mortar (WMRAMO) and WMRAM.

**Table 1. Comparison of research methods for evaluating fatigue properties of asphalt and asphalt mixtures**

Material	Test method	Advantages	Limitations
Asphalt <sup>20–22</sup>	Fatigue factor	Simple and easy to obtain	Only applicable to the linear viscoelastic stage
	Time sweep	Extensive applicability	Uncertain test duration
	Linear amplitude sweep test	Wide applicability and high accuracy	Complex calculation process
	Multiple-stress creep recovery tests	The load response of the recoverable and unrecoverable parts can be separated	Mainly used to evaluate permanent deformation
Asphalt mixture <sup>23–25</sup>	Fatigue bending test	Simple operation, mature equipment, stable results	The evaluation indicators need to be improved
	Fatigue test under direct tension	Extensive applicability	High equipment requirements; require test operations
	Splitting fatigue test	Test instrument operation, data stability	The failure mode and pavement service mode are different
	Semi-circular bending fatigue test	Wide applicability, simple operation	Inaccurate calculation process

Characterization methods for the fatigue performance of asphalt and asphalt mixtures include phenomenological, fracture mechanics, energy dissipation, and damage mechanics approaches.<sup>26,27</sup> Each method focuses on different aspects and has distinct application scopes. Because the fatigue failure of asphalt and asphalt mixtures is a process of damage accumulation, it is more advantageous to use damage mechanics to characterize it.<sup>28–30</sup>

Based on the literature review, to clarify the differences in fatigue properties between WMRAM and hot-mix asphalt mixtures, as well as the influence of material composition on WMRAM, this study examined the fatigue failure processes of WMRA, WMRAM, and WMRAMO materials at three scales, using SBSMAM as the control group. The correlations between fatigue parameters of the three materials were analyzed, differences in fatigue properties between WMRAM and SBSMAM were identified, and the effects of RAP content were elucidated. Additionally, a correlation model for fatigue life, incorporating strain and RAP content, was developed for WMRAMO and WMRAM. This work provides a scientific basis for the design optimization and further application of WMRAM.

## 2. Materials and methods

### 2.1. Materials

#### 2.1.1. Matrix asphalt and warm-mix rejuvenator

The base asphalt used was No. 90 petroleum asphalt, commonly used in road construction in northern China. The aged asphalt was extracted from RAP using centrifugal separation and the Abson method. The warm-mix rejuvenator used was styreneic methyl copolymers (SMC), primarily composed of hydrocarbons and resin materials. The technical indicators of the base asphalt and SMC are shown in Tables 2 and 3, respectively.

Table 2. Technical specifications of the base asphalt

Asphalt type	Technical requirement		
	Penetration (25 °C, 100 g, 5 s/0.1 mm)	Softening point (°C)	Ductility (15 °C/cm)
Matrix asphalt	97.6	47.63	>100
Aged asphalt	22.2	69.10	6.3

Table 3. Technical specifications of styreneic methyl copolymers

Parameter	Value
Density (25 °C, g/cm <sup>3</sup> )	0.962
Brookfield viscosity (100 °C, Pa·s)	0.85
Flash point (°C)	155

#### 2.1.2. Mineral mixture and reclaimed asphalt pavement

The new aggregate used in the test was basalt, and the mineral powder was limestone. The particle size of RAP was divided into three grades, and the specific parameters are shown in Table 4. The asphalt content of RAP was obtained using the combustion furnace method.

Table 4. Composition of reclaimed asphalt pavement

Aggregate size (mm)	Aggregate content (%)	Asphalt content (%)
10–20	97.8	2.2
5–10	97.3	2.7
0–5	94.2	5.8

#### 2.1.3. Warm-mix recycled asphalt

To facilitate analysis of the correlation between asphalt and mixture, the proportions of matrix asphalt, aged asphalt, and SMC in the recycled asphalt used in this study were inversely calculated based on the recycled asphalt mixture composition. The asphalt types used in the test included: asphalt (0%-O), corresponding to the asphalt mixture with 0% RAP content (0-YY; which is a hot-mix asphalt mixture, where YY refers to the original test piece); recycled asphalt 30%-O, corresponding to the asphalt mixture with 30% RAP content (30-YY); recycled asphalt 50%-O, corresponding to the asphalt mixture with 50% RAP content (50-YY); and recycled asphalt 70%-O, corresponding to the asphalt mixture with 70% RAP content (70-YY). The formulations of matrix asphalt, aged asphalt, and SMC in WMRA are shown in Table 5.

**Table 5. Formulations of warm-mix recycled asphalt (WMRA)**

Component	WMRA			
	0%-O	30%-O	50%-O	70%-O
Matrix asphalt (%)	100	68.0	49.6	46.5
Aged asphalt (%)	0	22.5	43.5	47.0
Styreneic methyl copolymer (%)	0	9.5	6.9	6.5

**2.1.4. Warm-mix recycled asphalt mixture**

The gradation curve of the mineral mixture for WMRAM is shown in Figure 1.

**2.1.5. Warm-mix recycled asphalt mortar**

There was no design specification for mortar in this study. Therefore, the mineral composition and asphalt content of mortar were calculated by referring to the corresponding asphalt mixture. In this study, the maximum particle size of the mortar was 5 mm, and the mineral mixture design was controlled using key sieves. Based on the target gradation and iterative trial adjustments, the control sieves were set to 2.360 mm, 0.600 mm, and 0.075 mm. By adjusting the proportions of each block material composition, RAP contents of 0% (0-RAP), 30% (30-RAP), 50% (50-RAP),

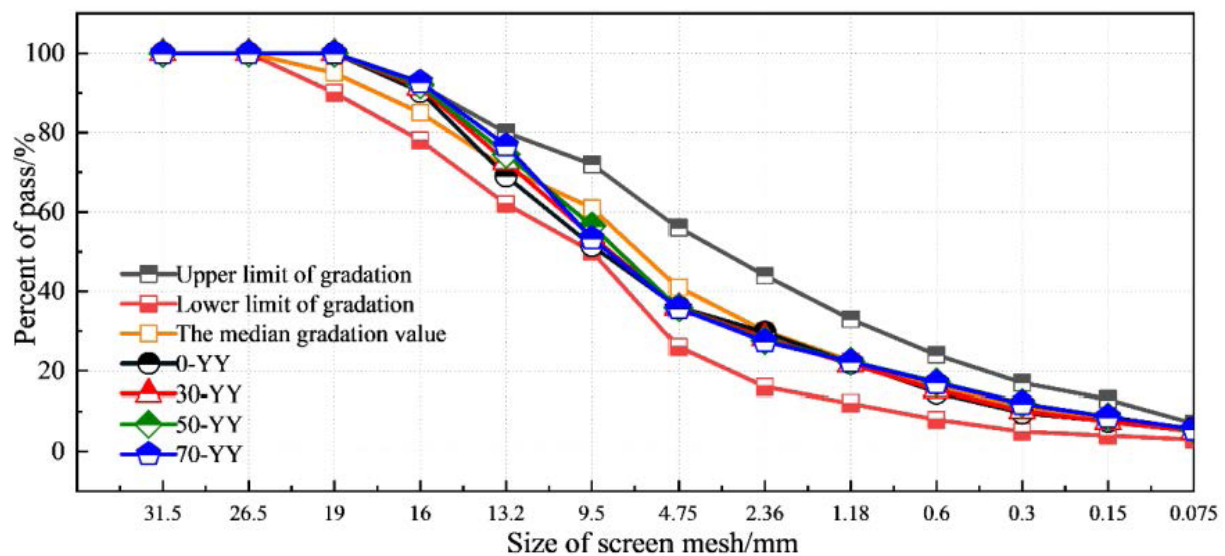
and 70% (70-RAP) were acquired.

**2.2. Fatigue test****2.2.1. Linear amplitude sweep test for asphalt**

The LAS test consists of two parts: frequency scanning and amplitude scanning. The test temperatures of the two parts were the same at 15 °C. The frequency scanning range was 0.2–30 Hz with a strain level of 0.1%. The loading frequency of amplitude scanning was 10 Hz, and the amplitude increased linearly from 0.1% to 30%.

**2.2.2. Four-point bending fatigue test for warm-mix recycled asphalt mortar and mixtures**

To facilitate a comparative study of the fatigue performance of asphalt mortar and asphalt mixture, the fatigue test method for asphalt mortar adopted the same four-point bending fatigue test as used for asphalt mixtures. The test temperature was 15 °C, with a loading frequency of 10 Hz. According to pre-test results—where the stiffness modulus decreased to 50% after fatigue loading cycles ranging from 1,000 to 1,000,000 (data not shown)—the loading strains for WMRAM were selected as 500  $\mu\epsilon$ , 600  $\mu\epsilon$ , and 700  $\mu\epsilon$ . For WMRMO, a single loading strain of 900  $\mu\epsilon$  was used. This study only considers the correlation between WMRMO and WMRAM and does not analyze the strain-dependent variation of WMRMO. Therefore, only one fatigue test under strain control was conducted. When comparing with WMRMO, a loading strain of 600  $\mu\epsilon$  was used for WMRAM. The tests were conducted using a UTM-100 testing machine (IPC Global, Australia)

**Figure 1. Proportions of the mineral mixtures**

equipped with a four-point bending pneumatic fixture.

### 2.2.3. Freeze–thaw test

The solutions used in this study were plain water and an 8% salt solution by mass concentration. Before the freeze–thaw cycles, the specimens were soaked in water. After soaking, the specimens were placed in containers filled with respective solutions and subjected to alternating high and low temperatures in the test chamber. The specimens were rapidly frozen at  $-20^{\circ}\text{C}$  for 4 h, followed by thawing at  $60^{\circ}\text{C}$  for 4 h. The number of freeze–thaw cycles was set to 10 (labeled as S10 for group soaking in water and Y10 for salt solution) and 20 (S20 for water and Y20 for salt solution).

## 3. Results and discussion

### 3.1. Determination of evaluation index

Since the final application scenario of warm-mix recycling technology of asphalt pavement is WMRAM, the fatigue indices of asphalt and asphalt mortar should be correlated with those of the asphalt mixture.

There are various methods to evaluate the fatigue performance of asphalt based on the LAS test, with evaluation indices calculated using damage mechanics. The most effective indices include the peak strain of virtual strain storage energy of asphalt ( $\varepsilon_p^W$ ) and the peak strain of the damage factor ( $\varepsilon_p^S$ ).  $\varepsilon_p^W$  corresponds to the time of microcrack nucleation, while  $\varepsilon_p^S$  corresponds to the time of microcrack coalescence. The calculation procedures and detailed explanations of these indices are described in detail in previous studies.<sup>29</sup>

In this study, the fatigue failure test methods for WMRAMO and WMRAM were identical, so the evaluation indices used were also the same. These indices included the number of loading cycles corresponding to a 50% reduction in stiffness modulus ( $N_f-D_{50}$ ), to a 50% reduction in virtual strain energy storage modulus ( $N_f-W_{50}$ ), and to the formation of microcracks ( $N_l$ ).<sup>31</sup> Both  $N_f-D_{50}$  and  $N_f-W_{50}$  serve as measures of fatigue life for WMRAM and WMRAMO.  $N_f-D_{50}$  can be directly observed at the end of the test, whereas  $N_f-W_{50}$  must be calculated based on the virtual strain energy storage. The calculation equations are as follows:

$$W^R = \frac{I}{2} C(S) (\varepsilon^R)^2 \quad (1)$$

where  $W^R$  is the virtual strain energy storage,  $\varepsilon^R$  is the strain, and  $C(S)$  is the virtual modulus, which is a function of the damage factor  $S$ . The expression for  $C(S)$  is as follows:

$$C(S) = \frac{\tau^p}{\varepsilon_p^R \times I} \quad (2)$$

where  $\tau^p$  is the stress amplitude,  $\varepsilon_p^R$  is the virtual strain amplitude, and  $I$  is the initial stiffness parameter, which is the ratio of the modulus of the first loading cycle to the modulus in the undamaged state. This parameter was introduced to reduce the variability between parallel specimens and is generally necessary to be between 0.9 and 1.1.

$$\varepsilon_p^R = \frac{1}{E^R} \times \varepsilon_p \times |G^*|_{lve} \quad (3)$$

where  $\varepsilon_p$  is the strain amplitude, and  $G^*$  is the complex shear modulus.

$N_l$  is determined by the energy ratio ( $R_l$ ) curve (Figure 2), though identifying the boundary between the first and second stages of the energy ratio can be challenging. This study introduced an innovation by analyzing the first derivative ( $S_R$ ) of the curve in Figure 2. It was found that the distribution of the first derivative exhibited a significant change at the boundary between the first and second stages. As shown in Figure 3, the number of loading cycles corresponding to this point of sudden change can be easily identified and corresponds to  $N_l$ .

### 3.2. Correlation analysis

#### 3.2.1. Correlation between microcrack formation and fatigue life of warm-mix recycled asphalt mixture

In theory, the earlier microcracks form in an asphalt mixture, the sooner fatigue damage is likely to occur. Therefore, the relationship between  $N_l$  and the fatigue life indicators  $N_f-D_{50}$  and  $N_f-W_{50}$  of WMRAM was analyzed (Figure 4). It can be seen from the figure that  $N_l$  has a significant correlation with both  $N_f-D_{50}$  and  $N_f-W_{50}$ . From the correlation coefficients ( $R^2$ ), the correlation between  $N_l$  and  $N_f-W_{50}$  was stronger than that with  $N_f-D_{50}$ . When RAP contents were low (0 and 30%), the correlations were basically linear, with  $R^2$  values exceeding 90%. However, as RAP content increased, the linear correlation weakened. When the RAP contents were higher than 50%,  $R^2$  dropped below 90%, mainly due to RAP variability. In the process of forming WMRAM, RAP did not fully act as a new aggregate and retained a part of the original damage. In addition, the variability of RAP (often considered a “black stone” rather than a stone) introduced uncertainty in the mineral mix ratio of the fresh mixture. Therefore, the factors that lead to fatigue failure increased, and the relationship between  $N_f-D_{50}$ ,  $N_f-W_{50}$ , and  $N_l$  was no longer



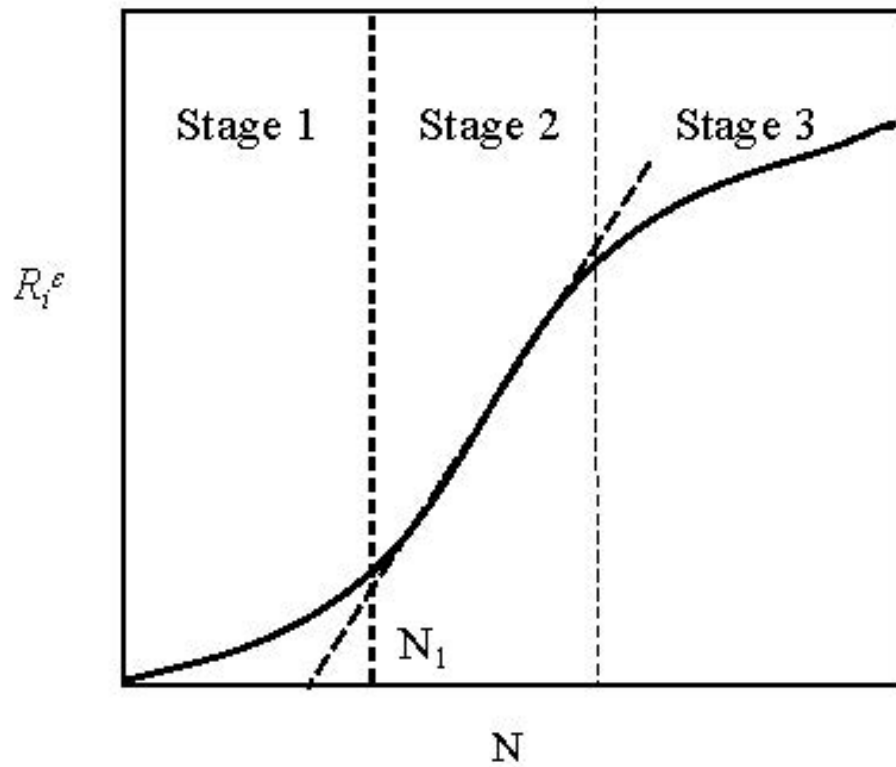


Figure 2. Changes in energy ratio ( $R_e$ ) with the number of cycles ( $N$ )

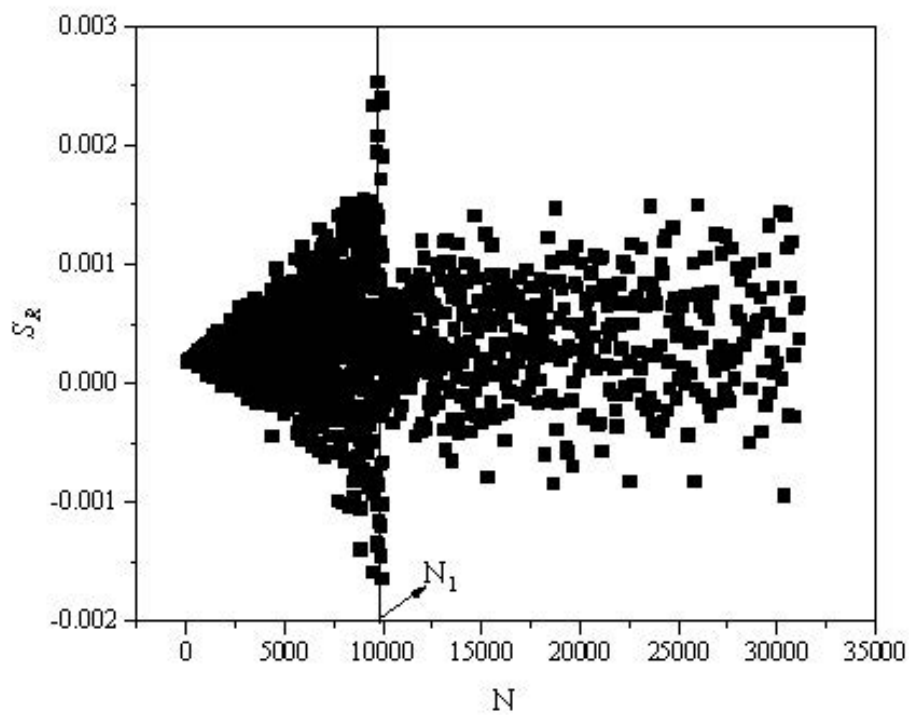


Figure 3. Changes in the first derivative ( $S_e$ ) with the number of cycles ( $N$ )

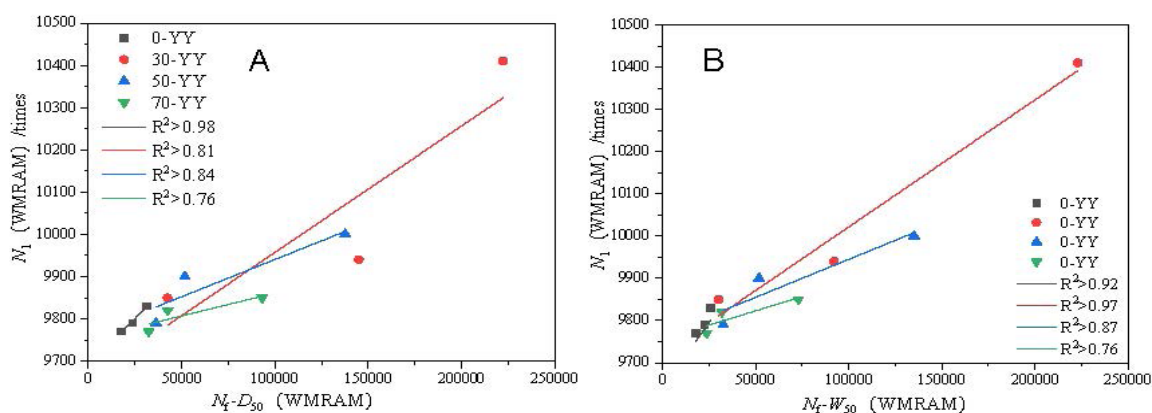


Figure 4. Correlation between microcrack formation ( $N_f$ ) and fatigue lives of warm-mix recycled asphalt mixture (WGRAM): (A)  $N_f-D_{50}$  and (B)  $N_f-W_{50}$

strictly linear.

In summary, the existence of RAP introduces more uncertainty into the process of microcrack development to fatigue failure in asphalt mixtures. For WGRAM with high RAP contents, predicting fatigue life based on microcrack formation needs to consider the variability of RAP, which markedly increases the difficulty of accurate prediction.

### 3.2.2. Correlation between the fatigue life of warm-mix recycled asphalt mixture and mortar

In this study, three considerations motivated the mortar fatigue-test design. First, a four-point bending fatigue test was adopted instead of a rheological test, which is easier to operate. The reason was that the sieve sizes of RAP and new aggregates differed during production. The minimum grade of RAP was 0–5 mm; therefore, the maximum particle size of the asphalt mortar was also set to 5 mm, resulting in relatively high material strength. The torque capacity of a dynamic shear rheometer (DSR) was insufficient to conduct reliable shear tests on mortar with this particle size, whereas mortars studied using DSR in previous studies typically have particle sizes of 0–3 mm.

Second, the four-point bending fatigue test matches the mixture fatigue-test configuration and facilitates correlation analysis. Third, for asphalt mortars, the skeleton structure effect was less obvious than that of the mixture, resulting in a lower probability of abrupt changes in stress and deformation fields during specimen failure. Consequently, the experimental data exhibited reduced variability. For example, in this experiment, a stable stiffness modulus–cycle number relationship could be obtained using two WGRAMO specimens, whereas at least three parallel specimens were required for WGRAM testing according to American Association of State Highway and Transportation Officials. Therefore, if asphalt-mortar

fatigue life correlates strongly with asphalt-mixture fatigue life, mortar tests could be used as a surrogate, greatly reducing experimental workload.

To analyze whether a correlation exists between the fatigue lives of WGRAMO and WGRAM, the  $N_f-D_{50}$  and  $N_f-W_{50}$  of both materials are plotted (Figure 5). It can be seen from the figure that the fatigue lives of WGRAMO and WGRAM exhibited a strong linear correlation, with  $R^2$  higher than 85% and a high degree of agreement between the experimental data points and the fitted lines. In addition, the slopes of the fitted linear relationships followed the order: 0-YY > 70-YY > 50-YY > 30-YY. The 0-YY specimen was a hot-mix asphalt mixture and differed from the other three specimens in terms of strength formation and fatigue failure mechanisms. When considering only the warm-mix recycled specimens, the slope decreased with increasing RAP content. Based on these observations, Equation 4 was employed to predict the fatigue life of WGRAM using the fatigue life of WGRAMO:

$$N_f^H = a \cdot p^b \cdot \varepsilon_r^c \cdot N_f^S + d \quad (4)$$

where  $N_f^H$  is the fatigue life of the asphalt mixture,  $N_f^S$  is the fatigue life of the asphalt mortar,  $p$  is the RAP content,  $\varepsilon_r$  is the ratio of mixture strain to mortar strain, and  $b$ ,  $c$ , and  $d$  are fitting parameters. The results are shown in Tables 6 and 7.

It can be seen from Tables 6 and 7 that the trends of the calculated fatigue life values with respect to strain and RAP content were consistent with those of the measured values. The calculation errors for both fatigue life indicators were controlled within 27%, demonstrating that it is feasible to predict the fatigue life of WGRAM through the fatigue life of WGRAMO from the perspectives of stiffness

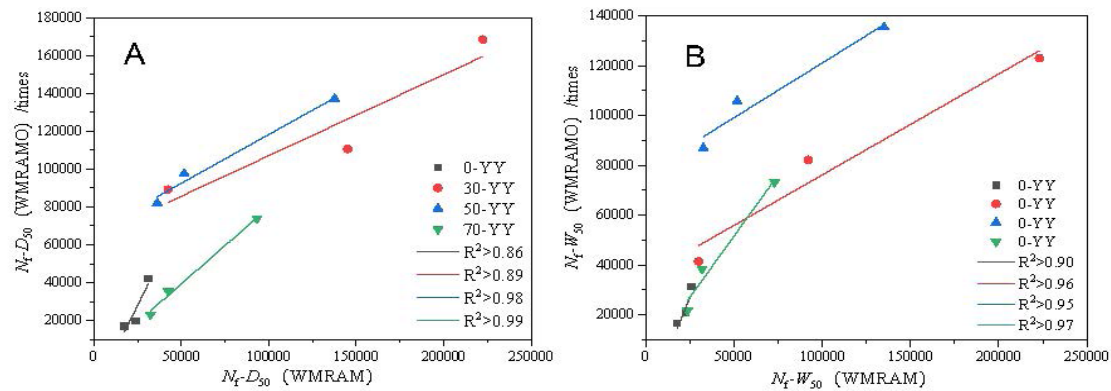


**Figure 5.** Correlation between the fatigue lives of warm-mix recycled asphalt mixture (WGRAM) and mortar (WGRAMO): (A)  $N_f-D_{50}$  and (B)  $N_f-W_{50}$

**Table 6.** Fatigue life prediction results based on  $N_f-D_{50}$

RAP content (%)	$\varepsilon_r$	$N_f-D_{50}$		Error (%)
		Measured value	Calculated value	
30	0.625	222,370	224,371	0.9
30	0.667	107,000	86,087	19.5
30	0.700	42,420	53,681	26.5
50	0.625	137,660	143,693	4.4
50	0.667	51,650	64,954	25.8
50	0.700	36,290	44,884	23.7
70	0.625	93,230	78,181	16.1
70	0.667	42,570	38,384	9.8
70	0.700	32,340	31,295	3.2

Abbreviation: RAP: Reclaimed asphalt pavement.

**Table 7.** Fatigue life prediction results based on  $N_f-W_{50}$

RAP content (%)	$\varepsilon_r$	$N_f-W_{50}$		Error (%)
		Measured value	Calculated value	
30	0.625	223,000	224,349	0.006
30	0.667	92,130	80,420	0.127
30	0.700	30,040	36,745	0.223
50	0.625	135,030	137,944	0.022
50	0.667	51,880	60,731	0.171
50	0.700	32,770	38,351	0.170
70	0.625	73,000	61,902	0.152
70	0.667	31,940	29,887	0.064
70	0.700	23,740	23,202	0.023

Abbreviation: RAP: Reclaimed asphalt pavement.



modulus and energy dissipation. Moreover, the fatigue life predictions based on energy dissipation calculation were more accurate. However, the fatigue lives of WMRAMO and WMRAM were affected not only by RAP content and control strain but also by intrinsic material properties. Therefore, there is still a gap between the predicted and measured fatigue lives.

### 3.2.3. Correlation between microcrack nucleation in warm-mix recycled asphalt and microcrack formation in warm-mix recycled asphalt mixture

The fatigue judgment index of asphalt in our previous study<sup>29</sup> was identified as a specific oscillating strain value that varies with different formulations. The peak strain of virtual strain energy storage corresponds to the failure strain of the nucleation of microcracks. The values of  $\varepsilon_p^W$  under different formulations and the  $N_f$  of the mixture are shown in Figure 6.

It can be seen from the figure that although the two parameters were derived from different materials, they exhibited a certain linear relationship, with an  $R^2$  of approximately 90%. However, at low strain, despite maintaining a strong correlation, the degree of dispersion between the data points and the fitted line was large. Therefore, the calculated values based on the established

mathematical correlation can have significant errors compared to the measured values. This discrepancy is attributed not only to the properties of the material but also to differences in test methods and the underlying theoretical bases of material damage. Therefore, no mathematical prediction formula was proposed in this study.

### 3.2.4. Correlation between microcrack nucleation in warm-mix recycled asphalt and fatigue life of warm-mix recycled asphalt mixture

The correlation between microcrack nucleation in WMRA and the fatigue life of WMRAM is plotted in Figure 7. From the diagram, it can be seen that the parameters of WMRA and WMRAM exhibited strong linear correlation when the strain was less than 600  $\mu\epsilon$ , particularly for  $N_f$ - $W_{50}$  and  $\varepsilon_p^W$ , with a high degree of agreement between data points and fitted lines. However, at 700  $\mu\epsilon$ , due to the high failure rate of WMRAM, the stiffness modulus and dissipated energy curves exhibited significant changes, leading to severe numerical fluctuations and a higher probability of sudden specimen failure. As a result, the correlation with WMRA-related indicators and the fit between points and lines deteriorated. Therefore, under the control strain adopted in this experiment, it is of little significance to establish a correlation equation between these parameters.

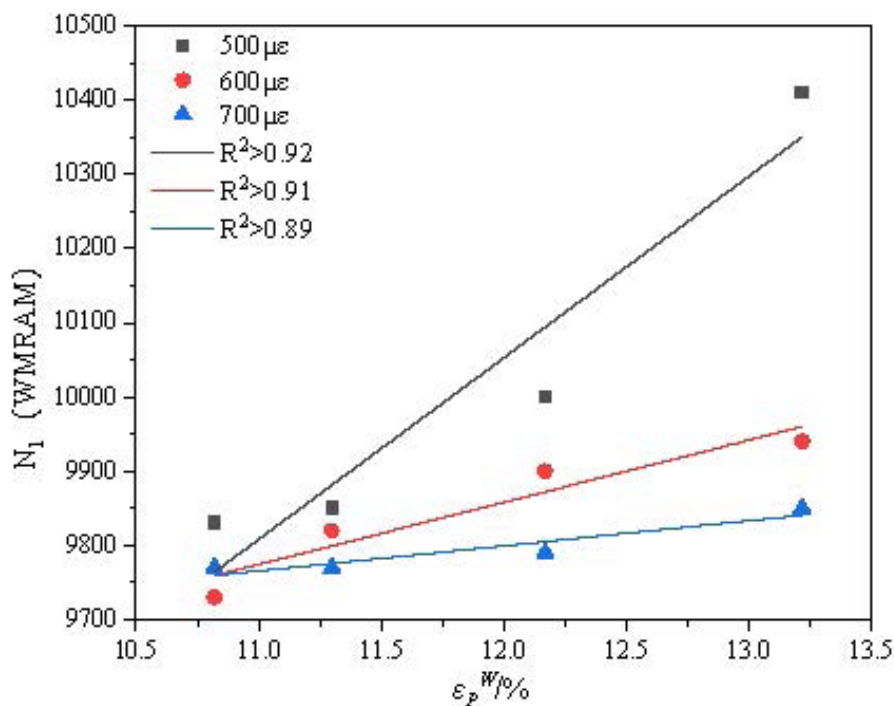


**Figure 6.** Relationship between microcrack nucleation ( $\varepsilon_p^W$ ) in warm-mix recycled asphalt and microcrack formation ( $N_f$ ) in warm-mix recycled asphalt mixture (WMRAM)

### 3.2.5. Correlation between the microcrack coalescence of warm-mix recycled asphalt and the fatigue life of warm-mix recycled asphalt mixture

Figure 8 shows the relationship between the peak strain corresponding to microcrack coalescence in WMRA and the fatigue life of WMRAM. It can be seen from the diagram that the overall trend was similar to the trend in Section 3.2.4. When the strain was low, the correlation between the parameters was strong. However, as the strain increased, the correlation weakened, and data dispersion grew. The correlation between  $N_f W_{50}$  and  $\varepsilon_p^S$  was slightly stronger than that between  $N_f D_{50}$  and  $\varepsilon_p^S$ . In addition, the correlations between  $\varepsilon_p^S$  and the two fatigue lives of WMRAM were lower than those between  $\varepsilon_p^W$  and the two fatigue lives. This is mainly due to the fact that the asphalt specimen remains undamaged before  $\varepsilon_p^W$ . During the transition from  $\varepsilon_p^W$  to  $\varepsilon_p^S$ , microdamage develops and progressively worsens. Consequently, the mechanical response of the material becomes less stable once damage initiates, increasing the variability of  $\varepsilon_p^S$  compared to  $\varepsilon_p^W$  and thereby reducing the correlation between  $\varepsilon_p^S$  and the fatigue life of WMRAM.

### 3.3. The impacts of freeze–thaw on fatigue properties

This section also uses  $N_f$ ,  $N_f W_{50}$ , and  $N_f D_{50}$  to evaluate changes in the fatigue performance of asphalt mortar and mixture after freeze–thaw cycles.

#### 3.3.1. Asphalt mortar

Figures 9 and 10 present the test results of  $N_f$ ,  $N_f W_{50}$ , and  $N_f D_{50}$  for asphalt mortar specimens before and after freeze–thaw cycles. The control strain of the freeze–thaw

specimen was determined to be 900  $\mu\text{e}$  according to the pre-test results (data not shown). All three parameters,  $N_f$ ,  $N_f W_{50}$ , and  $N_f D_{50}$ , decreased with increasing freeze–thaw cycles and higher salt solution concentrations. This decline is mainly due to frost heave effects and salt crystallization, which cause volume expansion that promotes the development of initial voids. Additionally, salt erosion reduces the adhesion between asphalt and aggregate, accelerating material damage progression and failure. In addition, these parameters continued to decrease with increasing RAP content after freeze–thaw cycles, consistent with pre-freeze–thaw trends, largely due to the differences and variability in RAP content.

For  $N_f$ , the 70-RAP WMRAM specimens after freeze–thaw cycles showed lower values than the matrix asphalt mortar specimens, indicating that microcracks in high-volume WMRAM specimens are more affected by freeze–thaw damage. This is due to the freeze–thaw process in which liquid water penetrates the material's pores; upon freezing, the water expands, generating frost heave forces that enlarge material voids and reduce structural integrity. The larger the initial void, the more water can infiltrate, intensifying the frost heave effect. WMRAM contains “black stone,” which refers to aged asphalt particles that have caused damage, such as fractures and voids, during service. During the warm-mix regeneration process, although the warm-mix regenerant softens the old asphalt and partially dissolves the “black stone,” it cannot fully eliminate this damaged material. Therefore, the initial voids and cracks of the WMRAM are larger than those of the matrix asphalt mixture, making it more susceptible to frost heave damage.

The variations of  $N_f W_{50}$  and  $N_f D_{50}$  with RAP content

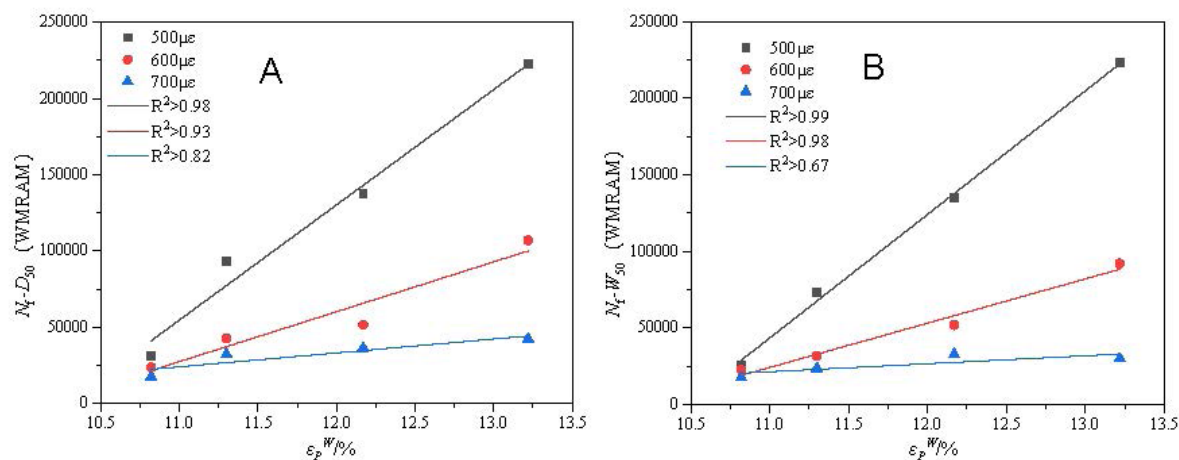
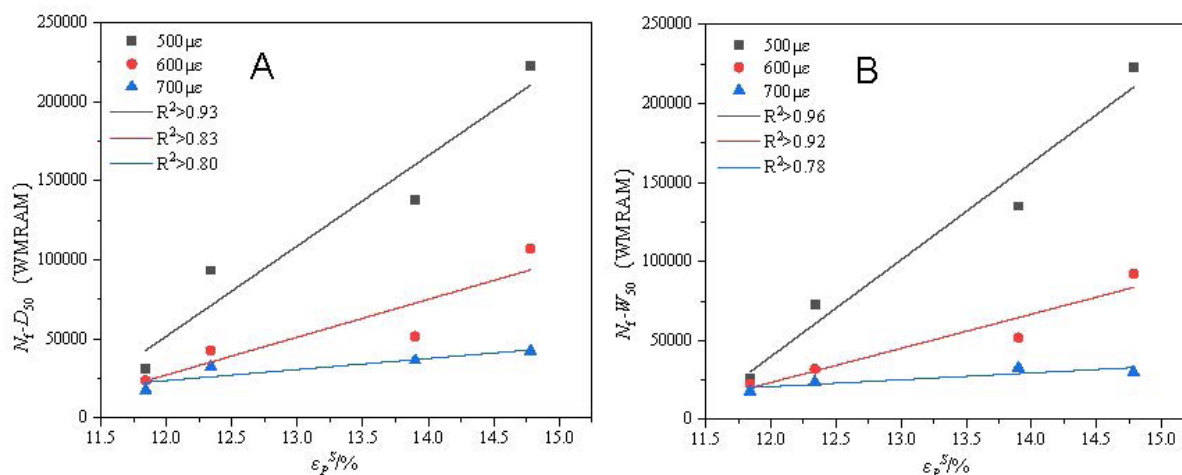


Figure 7. Relationship between microcrack nucleation ( $\varepsilon_p^W$ ) in warm-mix recycled asphalt and fatigue lives of warm-mix recycled asphalt mixture (WMRAM): (A)  $N_f D_{50}$  and (B)  $N_f W_{50}$



**Figure 8.** Relationship between microcrack coalescence ( $\varepsilon_p^S$ ) in warm-mix recycled asphalt and fatigue lives of warm-mix recycled asphalt mixture (WMRAM): (A)  $N_f-D_{50}$  and (B)  $N_f-W_{50}$

after freeze–thaw cycles were similar to those before freeze–thaw. However, the difference between  $N_f-W_{50}$  and  $N_f-D_{50}$  of 50-RAP specimens increased noticeably after freeze–thaw cycles. This discrepancy arises from their differing fatigue failure criteria:  $N_f-D_{50}$  is based on stiffness-modulus reduction, whereas  $N_f-W_{50}$  is based on reduction in virtual strain energy storage. As microdamage accumulated or cracks expanded, the stress and strain absorbed per loading cycle decreased, leading to a more pronounced reduction in dissipation energy than in strength. Therefore, the required damage energy decreased more obviously than strength, causing a greater reduction in fatigue life.

In addition, the decrease in fatigue life of asphalt mortar under salt solution freeze–thaw conditions was greater than that under pure water freeze–thaw conditions. This is because, in addition to frost heave force caused by water-to-ice phase changes, salt solution freeze–thaw introduces salt erosion and salt crystallization effects. Salt erosion weakens the adhesion between asphalt and aggregate, resulting in asphalt spalling from aggregate surfaces. Meanwhile, salt crystallization, like frost heave, causes volumetric expansion as solid salt forms, accelerating microcrack propagation. Therefore, fatigue life of asphalt mortar specimens decreases more rapidly in salt solution freeze–thaw cycles compared to water freeze–thaw cycles.

### 3.3.2. Asphalt mixture

Figures 11 and 12 present the test results of  $N_f$ ,  $N_f-W_{50}$ ,

and  $N_f-D_{50}$  for asphalt mixture specimens under different freeze–thaw conditions. The control strain for the freeze–thaw asphalt mixture specimens was determined to be 600  $\mu\text{m}$  according to the pre-test results (data not shown). It can be seen that the changes of the three parameters with respect to RAP content, freeze–thaw cycles, and salt solution concentration were similar to those of asphalt mortar specimens. However, by comparing Figures 9–12, it can be found that the range of variation in data for asphalt mixture specimens after freeze–thaw was significantly greater than that of asphalt mortar specimens. This can be attributed to the fact that during freeze–thaw cycles, frost heave effects and salt crystallization cause expansion of initial voids, thereby reducing the durability of materials. Additionally, salt erosion reduces durability by weakening the adhesion between asphalt and aggregate at the interface. All three forms of damage require the infiltrating solution to penetrate the material through initial gaps. Therefore, the larger the initial gaps, the greater the effects of freeze–thaw cycles on the materials. Since asphalt mixtures have larger gaps than asphalt mortars, the decrease in fatigue lives is more significant in mixtures.

It can also be found from Figures 9–12 that for  $N_f$ , the values of S20 specimens were higher than Y10 for both asphalt mortars and asphalt mixtures. In contrast, the trends for  $N_f-W_{50}$  and  $N_f-D_{50}$  were opposite. This indicates that the number of freeze–thaw cycles and the concentration of salt solution affect microcrack formation and fatigue failure differently.

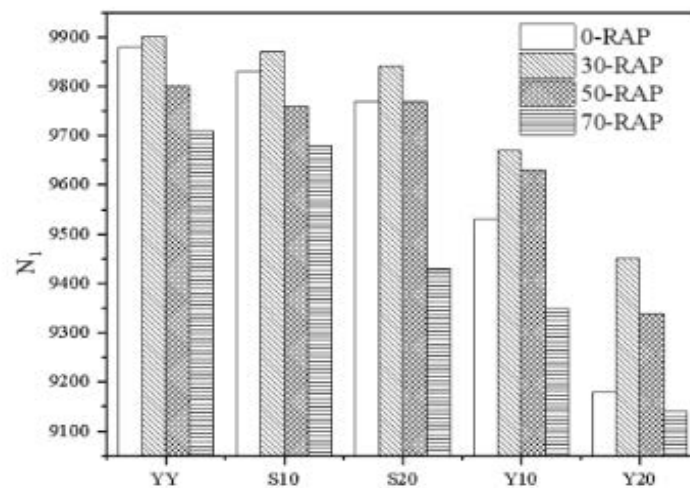


Figure 9. Microcrack formation ( $N_f$ ) of asphalt mortars before and after freeze–thaw cycles

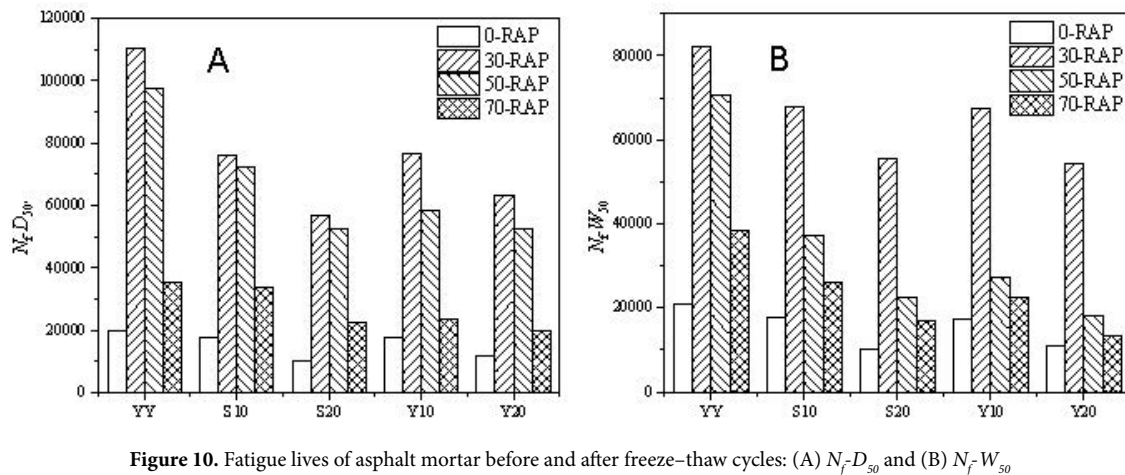


Figure 10. Fatigue lives of asphalt mortar before and after freeze–thaw cycles: (A)  $N_f D_{50}$  and (B)  $N_f W_{50}$

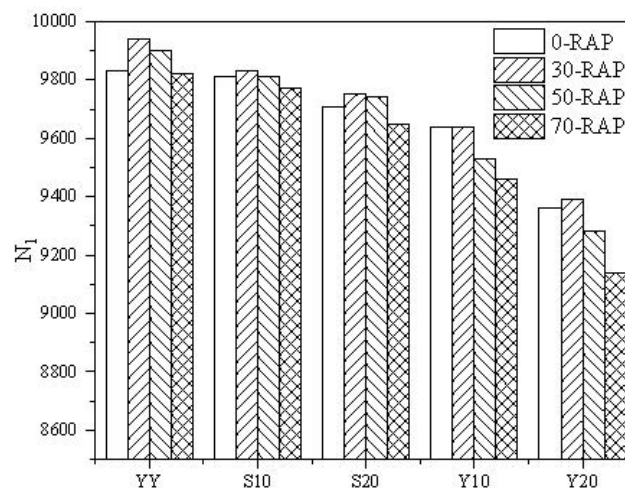


Figure 11. Microcrack formation ( $N_f$ ) of asphalt mixtures before and after freeze–thaw cycles

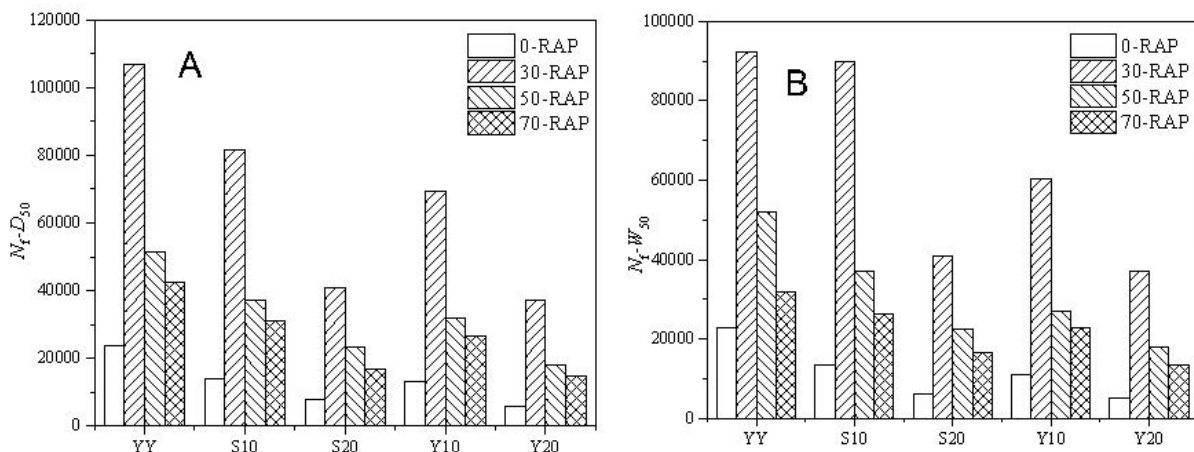


Figure 12. Fatigue lives of asphalt mixtures before and after freeze–thaw cycles: (A)  $N_f D_{30}$  and (B)  $N_f W_{50}$ .

## 4. Conclusion

This study systematically explored the fatigue properties of WMRAM under Asian-specific environmental conditions, yielding the following key conclusions:

- The mechanical parameters of WMRA, WMRAMO, and WMRAM under fatigue loading exhibited clear correlations; however, the strength of these correlations varied significantly depending on the loading method and RAP content.
- Laboratory tests showed that the fatigue lives of WMRAM could be predicted using the fatigue lives of WMRAMO under the same failure mode, provided that RAP content and loading strain were considered.
- Earlier nucleation of microcracks in WMRA corresponded to earlier microdamage in WMRAM and shorter fatigue lives, generally following a linear relationship. This indicated that damage development in WMRAM originated from WMRA and underscored the critical role of WMRA performance in the warm-mix regeneration process of asphalt pavement.
- Both microcrack initiation ( $N_i$ ) and fatigue life decreased with increasing freeze–thaw cycles and higher salt-solution concentrations. Notably, freeze–thaw cycles and salt solution concentration affected microcrack formation and fatigue failure differently.

This research provides a multi-scale framework for optimizing WMRAM design in Asia, bridging laboratory testing and field application while addressing the region's unique climatic challenges.

## Acknowledgments

None.

## Funding

This work was financially supported by a self-funded project of Inner Mongolia Power (Group) Co., Ltd, Inner Mongolia Power Research Institute (2024, Issue 114, 2024-ZC-2-08), and the Inner Mongolia Natural Science Foundation (2023LHMS05009).

## Conflict of interest

Wang Yu is affiliated with Inner Mongolia Power (Group) Co., Ltd, which partly funded this study. The funder had no role in study design; data collection, analysis, or interpretation; manuscript preparation; or the decision to publish. The authors declare no other competing interests.

## Author contributions

*Conceptualization:* All authors

*Formal analysis:* All authors

*Methodology:* All authors

*Writing – original draft:* All authors

*Writing – review & editing:* All authors

## Availability of data

Some or all data, models, or code that support the findings of this study are available from the corresponding author upon reasonable request.

## References

- Obaid HA, Enieb M, Eltwati A, *et al.* Prediction and optimization of asphalt mixtures performance containing reclaimed asphalt pavement materials and warm mix agents using response surface methodology. *Int J Pavement Res Technol.* 2024;1-17.
- Cui Y, Geng K, Zhou Q, *et al.* Research on the adhesion



- between warm mix recycled asphalt and aggregates at macro and micro scales. *Constr Build Mater.* 2024;455:139076.  
doi: 10.1016/j.conbuildmat.2024.139076
3. Zhang S, Cui Y, Du C, *et al.* Low-temperature performance and micro-structure of warm mix recycled composite aged asphalt. *Constr Build Mater.* 2024;440:137443.  
doi: 10.1016/j.conbuildmat.2024.137443
4. Phan TM, Choi YS, Youn SH, *et al.* Effect of synthesized warm mix additive and rejuvenator on performance of recycled warm asphalt mixtures. *Constr Build Mater.* 2024;421:135772.  
doi: 10.1016/j.conbuildmat.2024.135772
5. Sun J, Cheng Y, Zou G, *et al.* Study on the water stability and safety mechanism of warm mixed recycled SBS modified asphalt mixture. *Sci Rep.* 2025;15(1):31188.  
doi: 10.1038/s41598-025-31188-5
6. Zhang D, Liu Z, Xu P, *et al.* Recycling high-dosage SBS-modified Reclaimed Asphalt Pavement (RAP) into high-grade asphalt pavement based on a novel warm mix asphalt-synchronous rejuvenation (WMA-SR) technology. *Constr Build Mater.* 2025;472:140895.  
doi: 10.1016/j.conbuildmat.2025.140895
7. Liu J, Liu Q, Yin L, *et al.* Temperature and contact states of hot-recycled asphalt mixing at a non-thermal equilibrium condition based on discrete element method. *Constr Build Mater.* 2025;469:140526.  
doi: 10.1016/j.conbuildmat.2025.140526
8. Xing C, Li H, Chang Z, *et al.* A Comprehensive Review of Hot In-Place Recycling Technology: Classification, Factors Affecting Performance of Asphalt Mixtures, and Benefits Analysis. *Coatings.* 2025;15(7):794.  
doi: 10.3390/coatings15070794
9. Liu L, Sun L, Xu J, *et al.* Effect of RAP's preheating temperature on the secondary aging and performance of recycled asphalt mixtures containing high RAP content. *Constr Build Mater.* 2024;411:134719.  
doi: 10.1016/j.conbuildmat.2023.134719
10. Liu N, Liu L, Li M, *et al.* A comprehensive review of warm-mix asphalt mixtures: Mix design, construction temperatures determination, performance and life-cycle assessment. *Road Mater Pavement Des.* 2024;25(7):1381-1425.  
doi: 10.1080/14680629.2023.2253764
11. Carvalho JR, de Medeiros Melo Neto O, de Figueiredo Lopes Lucena AE, *et al.* Impact of adding warm asphalt mix additives on recycling milled coatings: performance evaluation. *Environ Sci Pollut Res.* 2024;31(58):66318-66349.  
doi: 10.1007/s11356-024-35594-8
12. Shu X, Huang B, Shrum ED, *et al.* Laboratory evaluation of moisture susceptibility of foamed warm mix asphalt containing high percentages of RAP. *Constr Build Mater.* 2012;35:125-130.  
doi: 10.1016/j.conbuildmat.2012.02.093
13. Zhao S, Huang B, Shu X, *et al.* Comparative evaluation of warm mix asphalt containing high percentages of reclaimed asphalt pavement. *Constr Build Mater.* 2013;44:92-100.  
doi: 10.1016/j.conbuildmat.2013.03.010
14. Alvarez DB, Kazmee H, Garg N. Laboratory and Field Performance Evaluation of Cracking of Airfield Warm Mix Asphalt with Reclaimed Asphalt Pavement at the National Airport Pavement and Materials Research Center. *Transp Res Rec.* 2024;2678(11):530-546.  
doi: 10.1177/03611981241257579
15. Sengoz B, Oylumluoglu J. Utilization of recycled asphalt concrete with different warm mix asphalt additives prepared with different penetration grades bitumen. *Constr Build Mater.* 2013;45:173-183.  
doi: 10.1016/j.conbuildmat.2013.03.077
16. Tang W, Sheng XJ, Xie XF, Zhou XL. The influence of recycled material content on the performance of warm mix recycled asphalt mixture. *J Build Mater.* 2016;19(1):204-208.
17. Wang HM, Yao S, Zhang Y, *et al.* Study on fatigue characteristics of hot mix and warm mix recycled asphalt mixture. *Highway Traffic Technology.* 2023;39(2):39-44.
18. Jiao L, Elkashef M, Harvey JT, *et al.* Investigation of fatigue performance of asphalt mixtures and FAM mixes with high recycled asphalt material contents. *Constr Build Mater.* 2022;314:125607.  
doi: 10.1016/j.conbuildmat.2021.125607
19. Qu L, Wang Y, Wang L, *et al.* Experimental evaluation of fatigue performance of recycled asphalt mixture using refined separation recycled aggregates. *Constr Build Mater.* 2024;411:134786.  
doi: 10.1016/j.conbuildmat.2023.134786
20. Steineder M, Peyer MJ, Hofko B, *et al.* Comparing different fatigue test methods at asphalt mastic level. *Mater Struct.* 2022;55(5):132.  
doi: 10.1617/s11527-022-01973-3
21. Zhou F, Mogawer W, Li H, *et al.* Evaluation of fatigue tests for characterizing asphalt binders. *J Mater Civ Eng.* 2013;25(5):610-617.  
doi: 10.1061/(ASCE)MT.1943-5533.0000671
22. Maggiore C. A comparison of different test and analysis methods for asphalt fatigue [dissertation]. University of Nottingham; 2014.
23. Guo Z, Wang L, Feng L, *et al.* Research on fatigue performance of composite crumb rubber modified asphalt mixture under

- freeze thaw cycles. *Constr Build Mater.* 2022;323:126603.  
doi: 10.1016/j.conbuildmat.2022.126603
24. Zhu C, Luo H, Tian W, *et al.* Investigation on fatigue performance of diatomite/basalt fiber composite modified asphalt mixture. *Polymers.* 2022;14(3):414.  
doi: 10.3390/polym14030414
25. Mousavi Rad S, Kamboozia N, Anupam K, *et al.* Experimental evaluation of the fatigue performance and self-healing behavior of nanomodified porous asphalt mixtures containing RAP materials under the aging condition and freeze–thaw cycle. *J Mater Civ Eng.* 2022;34(12):04022323.  
doi: 10.1061/(ASCE)MT.1943-5533.0004489
26. Zheng C, Cheng P, Li Y, *et al.* Measurement and characterization of asphalt fatigue behavior under multi-factor effects. *Mater Struct.* 2024;57(9):193.  
doi: 10.1617/s11527-024-02472-3
27. Ge D, Ju Z, Duan D, *et al.* Normalized fatigue properties of asphalt mixture at various temperatures. *J Road Eng.* 2023;3(3):279-287.  
doi: 10.1016/j.jreng.2023.08.001
28. Hu J, Wang L, Guo C, *et al.* Quantitative study on fatigue characteristics of warm mix recycled asphalt. *Constr Build Mater.* 2024;431:136532.  
doi: 10.1016/j.conbuildmat.2024.136532
29. He M, Yuan J, Zhu X. Fatigue damage characteristics and reliability analysis of asphalt mixtures using damage mechanics. *Constr Build Mater.* 2025;458:139748.  
doi: 10.1016/j.conbuildmat.2024.139748
30. Jin T, Yuan J, Peng X, *et al.* A fatigue damage model of asphalt mixture considering tensile and compressive modulus decay. *Case Stud Constr Mater.* 2024;20:e03133.  
doi: 10.1016/j.cscm.2024.e03133
31. Chowdhury PS, Noojilla SLA, Reddy MA. Evaluation of fatigue characteristics of asphalt mixtures using Cracking Tolerance index (CTIndex). *Constr Build Mater.* 2022;342:128030.  
doi: 10.1016/j.conbuildmat.2022.128030